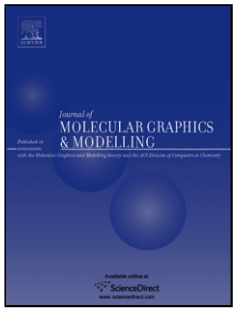

Title: Cloning and molecular modelling of a thermostable carboxylesterase from the chicken uropygial glands

Author: Ahmed Fendri Fakher Frikha Hanen Louati Madiha Bou Ali Hela Gargouri Youssef Gargouri Nabil Miled

PII: S1093-3263(14)00200-9
DOI: http://dx.doi.org/doi:10.1016/j.jmgm.2014.11.012
Reference: JMG 6491

To appear in: *Journal of Molecular Graphics and Modelling*

Received date: 4-8-2014
Revised date: 24-11-2014
Accepted date: 30-11-2014

Please cite this article as: A. Fendri, F. Frikha, H. Louati, M.B. Ali, H. Gargouri, Y. Gargouri, N. Miled, Cloning and molecular modelling of a thermostable carboxylesterase from the chicken uropygial glands, *Journal of Molecular Graphics and Modelling* (2014), http://dx.doi.org/10.1016/j.jmgm.2014.11.012

Graphical abstract:

The helices α1 (residues72-82) and α9 (residues 340-346) which are located on the top of the central β-sheet were proposed as potential lid and second lid, respectively. These two structural units (α1 and α9) may act as a double door controlling the access to the active site of the chicken uropygial carboxylesterase.

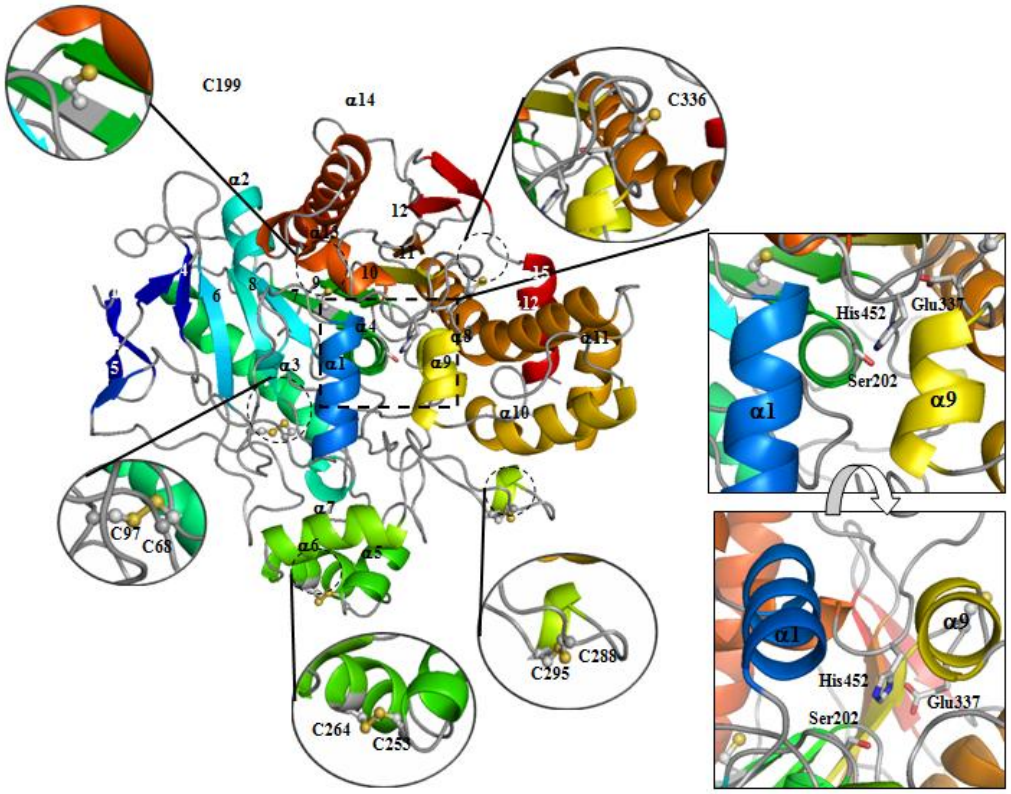

Highlights

- The chicken uropygial carboxylesterase (cuCES) cDNA was synthesized by RT-PCR.
- cuCES shows a high degree of homology with human liver carboxylesterase 1 (hCES1).
- A 3D structure model of the cuCES was built using the structure of hCES1 as template.
- Thermostability of cuCES was explained based on molecular dynamics (MD) simulations.
- Chicken CES could not accommodate large substrate molecule in its active site pocket.

Cloning and molecular modelling of a thermostable carboxylesterase from the chicken uropygial glands

Ahmed Fendri*, Fakher Frikha, Hanen Louati, Madiha Bou Ali, Hela Gargouri, Youssef Gargouri, Nabil Miled

Laboratoire de Biochimie et de Génie Enzymatique des Lipases, Ecole Nationale d'Ingénieurs de Sfax (ENIS), route de Soukra, BPW 3038 Sfax-Tunisia

*Correspondence address: Dr. Ahmed Fendri, Laboratoire de Biochimie et de Génie Enzymatique des Lipases, ENIS route de Soukra, 3038 Sfax-Tunisia. Tel/Fax: + 216 74675055, E-mail : Ahmed_ Fendri @yahoo.fr

Abbreviations

cuCES, chicken uropygial carboxylesterase; hCES1, human carboxylesterase 1; MD, molecular dynamics; RMSF, root-mean-square fluctuation;

Abstract

Starting from total uropygial glands mRNAs, chicken uropygial carboxylesterase (cuCES) cDNA was synthesized by RT-PCR and cloned into the PGEM-T vector. Amino acid sequence of the cuCES is compared to that of human liver carboxylesterase 1 (hCES1). Given the high amino acid sequence homology between the two enzymes, a 3-D structure model of the chicken carboxylesterase was built using the structure of hCES1 as template. By following this model and utilizing molecular dynamics (MD) simulations, the resistance of the chicken carboxylesterase at high temperatures could be explained. The docking of substrate analogues into the cuCES active site was used to explain the fact that the chicken carboxylesterase cannot hydrolyze efficiently large substrate molecules.

Key words: Chicken uropygial carboxylesterase; Nucleotide sequencing; 3D structure modelling; Thermostability; Molecular dynamic; Docking.

1. Introduction

Carboxylesterase (EC 3.1.1.1) is a class of enzymes that catalyze hydrolysis of the carboxyl ester bond. They prefer monoesters with short to medium acyl chains as a substrate. They are also able to hydrolyze short-chain triglycerides. Like lipases, carboxylesterases have broad substrate tolerance, high regio- and stereoselectivity, and stability in organic solvent, rendering them useful as biocatalysts for the synthesis of important bio-molecules [1].

Due to the relative abundance of these proteins and their involvement in chemical and pharmaceutical synthesis, synthesis of food ingredients and other various fields, many carboxylesterases (CES) have been purified to apparent homogeneity, and corresponding cDNAs were also isolated [2-4]. In addition, structures for human CES genes have been reported, including liver and intestinal enzymes (CES1 and CES2) genes [5-7].

Carboxylesterases belong to a superfamily of hydrolytic enzymes sharing a common structural framework namely the α/β hydrolyse fold [8]. The active site of these enzymes contains the same catalytic triad (Serine-Histidine-Aspartic/Glutamic acid) similar to that found in serine proteases. As in all serine hydrolases, the nucleophilic serine is part of a consensus peptide sequence Gly-X-Ser-X-Gly and catalysis proceeds via a two-step mechanism involving an acyl-enzyme intermediate.

Three dimensional structures for human CES1 have been determined at high resolution (2.8Å) [9-11] and three ligand binding sites have been described and designated as the active site, the side door, and the Z-site. The side door apparently assists with the release of the hydrolyzed product (eg. fatty acids) following catalysis, whereas the Z-site is supposed to play a role in regulating catalysis following ligand binding, and opening up the active site to substrate and subsequent catalysis [12]. Other key sites have also been identified in human CES1, based on the 3-D studies [9,10]: two disulfide bonds: Cys95/Cys123 and

Cys280/Cys291 and the 'gate' site which may facilitate product release following catalysis [9,10,12].

Recently, a carboxylesterase was purified from the chicken uropygial glands and some biochemical properties were determined [13]. The purified esterase displayed its maximal activity (200 U/mg) on short-chain triacylglycerols (tributyrin) at a temperature of 50°C and had no significant lipolytic activity on medium chain (trioctanoin) or long chain (olive oil) triacylglycerols.

In this work, we report the cloning of the chicken uropygial carboxylesterase (cuCES) cDNA and the comparison of the corresponding amino acid sequence with that of human liver carboxylesterase 1 (hCES1). Molecular modelling of cuCES was used to explain the thermostability and the substrate specificity of this enzyme.

2. Materials and methods

2.1. Chemicals

All enzymes used in DNA manipulations were from Promega and Invitrogen; oligonuclotides were synthesised by Invitrogen.

2.2. Bacterial strains, plasmids and media

E. coli strain DH5α was used as a cloning host for the gene part encoding the mature lipase. *E. coli* strain was grown in Luria-Bertani medium, supplemented with 100 μg/ml ampicillin whenever plasmid maintenance was required. The plasmid PGEM-T Easy (Promega) was used as a cloning vector. PCR products were purified using Wizard PCR Preps DNA purification System (Promega).

2.3. cDNA synthesis and amplification

The coding sequence of cuCES was determined by reverse transcriptase-polymerase chain reaction (RT-PCR) and amplification of mRNA from chicken uropygial glands. Total mRNAs were isolated from chicken uropygial glands using the single step guanidine isothiocyanate-phenol-chloroform isolation method developed by Chomcznski and Sacchi [14]. cuCES cDNA was obtained from total mRNAs by the reverse transcription procedure (Promega).

First strand cDNAs were prepared using heat-denaturated (5 min at 70 °C) total mRNAs (10 μg) as template, 200U MMLV reverse transcriptase (Invitrogen), 20 *p*mol of each deoxynucleoside triphosphate, and 20 *p*mol of each primer, (forward primer, $^{5'}$AAAGCAGAGCAACCAGAA$^{3'}$; reverse primer, $^{5'}$TCACAAATCTGTGCGTTC$^{3'}$). Primers were predicted, respectively, from the N-terminal sequence of the purified cuCES and the C-terminal of an enzyme similar to a fatty acyl-CoA hydrolase precursor of *Gallus gallus* (GenBank accession no. **XM001232057**), chosen according to the high homology between the N-terminal sequence deduced from this hydrolase and that of cuCES.

Reverse transcription was carried out in a total reaction volume of 20 µl for 5 min at room temperature and then for 60 min at 42°C. The cDNA/RNA heteroduplex was then denaturated at 70°C for 15 min and cooled on ice.

2.4. Cloning of the mature esterase gene region

Amplification of the specific cuCES cDNA was carried out by PCR using the single strand cDNAs as template with primers, $^{5'}$AAAGCAGAGCAACCAGAA$^{3'}$, and $^{5'}$TCACAAATCTGTGCGTTC$^{3'}$. PCR was performed in a 0.2 ml eppendorf tube with a Gene Amp® PCR System 2700. The PCR mixture contained 20 *p*mol of both primers, 20 *p*mol of each deoxynucleoside triphosphate, polymerisation buffer, and 5 U Taq polymerase (Amersham Pharmacia Biotech) in 100 µl. The single strand cDNAs were directly used as template. The thermal profile involved 35 denaturing cycles at 94°C for 1 min, primer annealing at 55°C for 1 min, and extension at 72°C for 3 min.

The PCR product (1.7 kb) was isolated and ligated into the *EcoRI* linearised and dephosphorylated PGEM-T Easy vector, using the PGEM-T Easy blunt ended cloning kit, according to the manufacturer's protocol (Promega). Protoplasts of *E.Coli* DH5α were transformed with the ligation mixture. The resulting recombinant plasmid was named pCES. The presence of the appropriate insert was determinated by restriction analysis. DNA products were analysed on a standard 1 % agarose gel containing ethidium bromide (1µg/ml). DNA sequences were elucidated by the dideoxynucleotide chain termination method according to a cycle sequencing protocol using thermosequenase (Amersham Pharmacia Biotech). The DNA sequencing reactions were carried out at the Biotechnological Center of Sfax (Tunisia) with the DNA sequencer ABI PRISM 3100/3100-Avant Genetic Analyser (California, USA). The sequencing was performed three times, using the recombinant vector (pCES) as template with T7 promotor primer and the M13 reverse primer (Invitrogen).

2.5. Nucleotide sequence access number

The nucleotide sequence of mature CES, determined in this study, was deposited in the GenBank database under Accession No. **JQ714283**

2.6. Software for infrastructure:

The sequence alignment was performed with BioEdit Version 7.2.5 software [15]. The Molecular Operating Environment 2009.10 (MOE) software [16] was used for homology modelling, molecular dynamics and structures visualization. The models were stereochemically evaluated by the program PROCHECK [17]. The Visualization and figures generation were performed with PyMol program version 0.99beta06 [18].

2.7. Homology Modelling

The 3-D coordinates of the Human liver carboxylesterase 1 in complex with tocrine (hCES1) (PDB code: 1MX1) was extracted from the Protein Data Bank (http://www.rcsb.org). The hCES1 structure was used as template to build the model of the cuCES structure by using the structure-modelling program Molecular Operating Environment 2009.10. The model of the cuCES was then subjected to molecular mechanics optimization using CHARMM27 force field [19]. Energy minimization (geometry optimization) was performed until the gradient of 0.05 kcal/(Å.mol) was reached. The RMS deviations involving α-carbons between the initial and the optimized models were 1.36 Å.

2.8. Docking

The tributyrin (TC_4, short chain triacylglycerols) and trioctanoïn (TC_8, medium chain triacylglycerols) were modelled by the ChemBioDraw Ultra software v12.0 from CambridgeSoft. The Molegro Virtual Docker v.6.0.0 software [20] was used for docking substrates, TC_4 and TC_8 to the cuCES model.

The potential binding sites (also referred to as cavities or active sites) were being identified using the built-in cavity detection algorithm, molecular surface with 0.3 Å grid resolutions and 1.2 Å Probe size.

After preparation of the protein and the ligand, the docking was performed using MolDock Score function and MolDock SE search algorithm [20]. Ten runs of energy minimization were performed to optimize H-Bonds after docking. 2500 iterations and 500 steps Simplex Evolution were applied to generate the best five poses scores which were visually analyzed.

Only one of these poses corresponding to the highest score was used. The protein-substrate complex was then subjected to molecular mechanics optimization using CHARMM27 force field as described previously. The Score of the final protein-substrate complex was evaluated using the total interaction energy between the active site and the substrate.

2.9 Molecular dynamic simulations

Molecular dynamic simulations were carried out at 101 kPa using Nose´-Poincare´-Anderson equations of motion (NPA Algorithm) [21], rigid water and light bonds constrains, a relative accuracy of 1e-012, a time step of 0.002 ps, a temperature response of 0.2 ps and a pressure response of 5 ps. After minimization, the system heating, equilibration and data sampling were carried out for the cuCES model. The system heating was performed gradually from 0 to 310 K in a NVT ensemble (constants: N—number of particles, V—volume and T—temperature) and equilibrated for 100 ps, followed until 1 ns simulation for data sampling in a NPT ensemble (constant: N—number of particles, P—pressure and T—temperature) at 310K (37°C) and 330 K (57°C), respectively.

3. Results and discussion

3.1. Cloning and sequencing of the mature lipase gene region

Based on the N-terminal sequence of the purified chicken uropygial carboxylesterase [13] and the C-terminal sequence of an enzyme similar to a fatty acyl-CoA hydrolase precursor of *Gallus gallus* (GenBank accession no. **XM001232057**), the carboxylesterase cDNA was selectively amplified by RT-PCR from total RNAs isolated from chicken uropygial glands. A band of 1700 pb corresponding to carboxylesterase gene size was amplified. The carboxylesterase gene was cloned into the PGEM-T Easy vector. The insert sequence (Fig. 1) corresponds to the gene part encoding the mature cuCES. The deduced polypeptide sequence of cuCES, corresponding to the mature protein, comprises 549 amino acids. The amino acid sequence of mature cuCES was aligned to that of human liver carboxylesterase 1 (hCES1) (Fig. 2). cuCES shares 52 % of sequence identity with hCES1. Several key residues are conserved between cuCES and hCES1 (Fig. 2): The active site 'triad' (Ser202, Glu337 and His452) [22]; Gly339 known as the Z-site [9-11] which binds cholesterol-like compounds, Gly123-Gly124, which may be part of an oxyanion hole and disulfide bonds Cys68/Cys97 and Cys253/Cys264 (Fig. 2) [23]. Interestingly, cuCES possesses additional cystein residues (Cys199, Cys288, Cys295 and Cys336) that are not found in hCES1 sequence suggesting that chicken carboxylesterase may contain more disulfide bridges.

The N-glycosylation site for human CES1: Asn60-Ala61-Thr62 [9,10,24] was not present in the chicken uropygial CES sequence since Asn60 was replaced by an Asp residue. Another potential carbohydrate binding site was identified for cuCES sequence (Asn468-Ala469-Thr470) (Fig. 2).

Two charge clamps that are responsible for ionic subunit-subunit interaction are important for hCES1 activity: ion pairs Lys59/Glu164 and Glu53/Arg167, which contribute to

the trimeric and hexameric structures of the enzyme [9,10,12]. However, cuCES contains only one of these clamps (Arg167 binding to Glu53), whereas the second charge clamp (Glu164 binding to Lys59 in the hCES1) is absent due to the substitution of Glu164 by 164Lys. This fact would explain the monomeric state of cuCES [13].

Structural analysis of human CES1 allowed to identify a major ligand binding site, the 'side door' (residues Val408-Met409-Phe410), where substrates, fatty acids and cholesterol analogues, are embedded [9,10,12]. Met409 residue in human CES1 has been described as the most important residue when it comes to regulating the release of fatty acids following hydrolysis of esters. This residue serves as a 'gate' at the 'side door' of the enzyme's active site. Meanwhile, Phe410 acts as a 'switch' also in the 'side door' region [9-11]. Only Met409-Phe410 key residues are present in the 'side door' sequence of the cuCES (Fig. 2). This may reflect a change in the kinetics or specificity in the regulation fatty acid or other acyl-product release for cuCES compared to hCES1. The key residue in the human CES1 'gate', Phe535, is replaced by a Thr in cuCES sequence. The significance of this change in 'gate' residues for chicken CES remains to be determined. This change may influence product release following acyl hydrolysis or transesterifcation.

3.2. Homology Modelling

The structure model of the chicken uropygial carboxylesterase (cuCES) was built, using as template the crystal structure of the human liver carboxylesterase 1 (hCES1) in complex with tacrine (PDB code: 1MX1). The two carboxylesterases share an amino acid sequence identity of 52 % (Fig. 2). The Ramachandran plot statistics of the final cuCES model and of the hCES (template), determined using the PROCHECK program [17], showed that 97.2 %, and 99.8 % of the residues were in the favored and allowed regions, respectively.

3.3. Overall model structure and active site

The 3D structure model of cuCES has a globular shape with an α/β hydrolase fold common to several hydrolytic enzymes and similar to that present in all carboxylesterases 1 [8,25]. The structure shows a single compact domain that consists of 14 β-strands and 15 α-helices. The core structure consists of a central 11β-stranded β-sheet in the following order: β3-β4-β6-β8-β7-β9-β10-β11-β12-β13-β14 (strands β3, β6 and β14 are anti-parallel), surrounded by α-helices α2, α13 and α14 on one side and α-helices 3,4,5,6,7,8,10,11,12,13,15 and stands β1-β2-β5 on the other side [Fig. 3(a)].

The active site is located at the bottom of a 10-15 Å deep catalytic gorge surrounded by two loops (β12-α13 and α7-α8) and two helices (α1 and α9). Ser202, Glu337 and His452 in cuCES are positioned in a catalytic triad like configuration. The catalytic Ser202 is located in the nucleophilic elbow between strand β9 and helix α4 deep within the core structure (Fig. 3). The 3D structure model of cuCES contains two disulfide linkages (Cys68-Cys97 and Cys253-Cys264) which are conserved in hCES1 structure (Fig. 3). Interestingly, the cuCES model contains an additional disulfide bridge (Cys288-Cys295) and two free cysteins (Cys199 and Cys336), compared to hCES1. This fact might to contribute to enhancing the thermostability of this enzyme which retains 75 % of its activity after an incubation for 2 h at 50°C [13].

The 3D structure of hCES1 shows one high-mannose, N-linked glycosylation site on Asn79. The model of cuCES shows no N-linked glycosylation site on the corresponding position (Asn79 in hCES1 was replaced by Asp60). In cuCES, the Asn468 might be the first residue of an N-glycosylation site consensus pattern: N-{P}-[ST]-{P}. The corresponding sequence in cuCES (residues Asn468-Ala469-Thr470-Glu471) is located between helix α13 and α14. It was reported that the N-glycosylated carbohydrate group contributes to the

stability and maintaining catalytic efficiency of the human CES1 [24]. This potential glycosylation site might also contribute to enhancing the thermostability of the chicken CES.

3.4. Lid domain

The helices α1 (residues72-82) and α9 (residues 340-346) which are located on the top of the central β-sheet were proposed as potential lid and second lid, respectively. These two structural units (α1 and α9) may act as a double door controlling the access to the active site of the chicken CES [Fig 3(b) and 3(c)]. The accessible surface of the amino acids belonging to these two helices covering the active site is around 590 Å².

The inactivation of a lipase by phenylmethylsulfonyl fluoride (PMSF), in the absence of bile salts, was proposed as a criterion to identify lipases having an accessible active site in solution [26]. If the lid domain is absent or under its open form in solution, the PMSF molecules can reach the active site and react with the catalytic serine even in the absence of bile salts [26]. If the active site of a lipase is covered by a lid domain, the latter forms a barrier that prevents the access of the PMSF to the catalytic serine except when bile salts are added. The preincubation of PMSF with bile salts would yield mixed micelles that may induce opening of the lid and consequently chemical modification of the catalytic serine. The chicken carboxylesterase were found to be inactivated by the PMSF (1 mM final concentration) after preincubation for 60 min in the absence of bile salts [sodium deoxycholate (NaDC)] [13]. This result suggests that the catalytic serine of the cuCES is likely not fully covered by the two lids (helices α1 and α9). This finding is in line with the fact that cuCES displays a semi-covered active site [Fig. 3(b)].

3.5. Enzyme stability and flexibility

Carboxylesterases have a wide range of substrate specificity. They have the ability to hydrolyze xenobiotic esters and may be involved in the detoxification of drugs. However, it was also reported that some of these carboxylesterases could specifically hydrolyze lipids

such as palmitoyl-CoA, acyl-carnitine and mono and diacylglycerols. Because these lipids naturally exist in the uropygial gland, the carboxylesterase may have a functional role in the regulation of their concentration and participate in the turnover of these lipids. In addition, the chicken carboxylesterase could be involved in the hydrolysis of monoesters (the major wax compounds in the uropygial gland) to release medium chain fatty acids for the synthesis of di-esters whose level is enhanced by drugs and growth hormones treatments during avian breeding.

We have recently reported that chicken CES displays its maximal activity at high temperature (50°C). The key feature of an enzyme function is the maintenance of an appropriate balance between molecular stability and structural flexibility. The lid domain is the most flexible part in the lipase structure that regulates the access to the enzyme active site [27]. Moreover, Gatti-Lafranconi et al [28] reported that the enzyme's stability was enhanced by restriction of the lid mobility. We analysed the possible interactions connecting the lid helix and the rest of the protein. Our results show that amino acids residues of the two helical lids of cuCES are involved in 29 interactions with the protein core. Most of them (21 interactions) are hydrophobic contacts. However, only 22 interactions are found in the case of the human CES1 which is more active at 37°C [29]. According to these observations, thermoactivity of the chicken CES may be attributed to the restriction of its lid's mobility due to strong interactions with the protein core.

In order to explain the thermostability of the cuCES, we used molecular dynamics (MD) simulations. The closed to open conformation transition were traced under different temperatures. Transition from an open and to a closed conformation was investigated by MD simulations for lipases of: *Candida Antarctica* [30], *Pseudomonas aeruginosa* [31], *Candida rugosa*, *Bacillus subtilis* [32], *Burkholderia cepacia* [33,34], *Yarrowia lipolytica* [35], *Rhizomucor miehei* and *Thermomyces lanuginose* [36]. Molecular dynamics simulations (1

ns) were carried out for the cuCES model at medium (37°C) and high (57°C) temperatures. The root-mean-square fluctuation (RMSF) values for the backbone atoms were calculated as a function of simulation time to understand the residue flexibility (Fig. 4). Average RMSF values in the MD simulations are usually considered as the criterion for overall flexibility of a system [37]. RMSFs of the backbone atoms were calculated for each residue over the last 900 ps of MD simulation time. Results clearly revealed that the enzyme's flexibility was slightly affected by increasing temperature from 37 to 57°C (Fig. 4). This is consistent with the thermostability of the chicken carboxylesterase. Nevertheless, significant differences were observed in the lid region. Root mean square fluctuations (RMSF) of C_α (Fig. 4) revealed significant local flexibility at 37 and 57°C, for residues 72–82, which are located in the lid helix α1. The flexibility at helix lid α1 is much higher at 57°C rather than at 37°C. Moreover, a slight increase in fluctuations was observed for residues 340-342, which are located in the second lid (helix α9). This distinct reorientation in the two lids suggests a conformational change towards lids opening. At a high temperature, the catalytic triad may be more exposed to the substrate. This could explain why chicken CES is more active at 50°C [13].

3.6. Docking

Analysis of the chicken CES structure bound to a substrate can help understand the interaction mode of the substrate once located in the catalytic pocket.

The docking of substrate analogues, propane-1,2,3-triyl tributyrate (analogue of tributyrin) and propane-1,2,3-triyl trioctanoate (analogue of trioctanoïn) into the cuCES active site, was performed using the Molegro Virtual Docker v.6.0.0 software.

The substrate binding gorge of the cuCES consists mainly of residues: Leu78, Phe82, Gly123, Gly124, Leu127, Ser202, Arg233, Thr283, Ser299, Phe301, Glu337, Ile342, Met345, Phe372, Met409 and His452. Catalytic triad residues (Ser202, Glu337 and His452) are located at the bottom of this gorge.

According to the protein-substrate complexes, 28 and 22 residues of cuCES active site are in van der Waals contacts with trioctanoïn (TC_8) and tributyrin (TC_4) analogues, respectively. Key residues of the catalytic triad (Ser202 and His454) interact with the carbonyl group of the substrate analogue docked into the active site. Key residue Gly124 belonging to the oxyanion hole seems to stabilize the nucleophilic oxygen of the substrate during the catalytic mechanism (Fig. 5). The active site gorge of the cuCES has a molecular volume of about 446 $Å^3$ which is higher than that of TC_4 analogue (283 $Å^3$) and smaller than that of TC_8 analogue (471 $Å^3$). This fact suggests that the chicken carboxylesterase has a preference for small substrate molecules. The lack of cuCES activity on medium and long chain triacylglycerols might be further attributed to a regulation of the lid opening by the interface quality as it was suggested in the case of other esterases [38].

Conclusion

The chicken uropygial carboxylesterase (cuCES) sequence shows a high degree of homology with that of human liver carboxylesterase 1. cuCES is characterized by its thermostability. This fact was explained, based on a 3-D structure model that showed an additional disulfide bridge when compared to human CES1 and a low flexibility of lid domains at high temperature. The chicken CES could not accommodate large substrate molecule in its active site pocket. This might partly explain the inability of the enzyme to hydrolyze medium or long chain triacylglycerols. Further studies on the interactions of enzymes with various interfaces would help understand its lack of activity on medium and long chain triacylglycerols.

Acknowledgments

We are grateful to Ms E. Karray for her help with the English. This work received financial support from the Tunisian Ministry of Higher Education and Scientific Research granted to the « Laboratoire de Biochimie et de Génie Enzymatique des Lipases ».

References

1. Bornscheuer UT. Microbial carboxyl esterases: classification, properties and application in biocatalysis. FEMS Microbiol rev 2002;26:73–81.

2. Munger JS, Shi GP, Mark EA, Chin DT, Gerard C, Chapman HA. A serine esterase released by human alveolar macrophages is closely related to liver microsomal carboxylesterases. J Biol Chem 1991;266:18832-18838.

3. Ovnic M, Tepperman K, Medda S, Elliott RW, Stephenson DA, Grant SG, Ganschow RE. Characterization of a murine cDNA encoding a member of the carboxylesterase multigene family. Genomics 1991;9:344-354.

4. Alexson SEH, Finlay TH, Hellman U, Svensson LT, Diczfalusy R, Eggertsen G. Molecular cloning and identification of a rat serum carboxylesterase expressed in the liver. J Biol Chem 1994;269:17118-17124.

5. Ghosh S. Cholesteryl ester hydrolase in human monocyte/macrophage: cloning, sequencing and expression of full-length cDNA. Physiol Genomics 2000;2:1–8.

6. Langmann T, Becker A, Aslanidis C, Notka F, Ulrich H, Schwer H, Schmitz G. Structural organization and characterization of the promoter region of a human carboxylesterase gene. Biochim Biophys Acta 1997;1350:65–74.

7. Marsh S, Xiao M, Yu J, Ahluwalia R, Minton M, Freimuth RR, Kwok PY, McLeod HL. Pharmacogenomic assessment of carboxylesterases 1 and 2. Genomics 2004;84:661–668.

8. Lenfant N, Hotelier T, Bourne Y, Marchot P, Chatonnet A, Proteins with an alpha/beta hydrolase fold: relationships between subfamilies in an ever-growing superfamily. Chem Biol Interact 2013;203:266–268.

9. Bencharit S, Edwards CC, Morton CL, Howard-Williams EL, Kuhn P, Potter PM, Redinbo MR. Multisite promiscuity in the processing of endogenous substrates by human carboxylesterase 1. J Mol Biol 2006;363:201-214.

10. Bencharit S, Morton CL, Xue Y, Potter PM, Redinbo MR. Structural basis of heroin and cocaine metabolism by a promiscuous human drug-processing enzyme. Nature Struct Biol 2003;10:349-356.

11. Redinbo MR, Potter PM. Mammalian carboxylesterases: from drug targets to protein therapeutics. Drug Discov Today 2005;10:313-320.

12. Fleming CD, Bencharit S, Edwards CC, Hyatt JL, Trurkan L, Bai B, Fraga C, Morton CL, Howard-Williams EL, Potter PM, Redinbo MR. Structural insights into drug processing by human carboxylesterase 1: tamoxifen, Mevaststin, and inhibition by Benzil. J Mol Biol 2005;352:165-177.

13. Fendri A, Louati H, Sellami M, Gargouri H, Smichi N, Zarai Z, Aissa I, Miled N, Gargouri Y. A thermoactive uropygial esterase from chicken: Purification, characterisation and synthesis of flavour esters. Int J Biol Macro 2012;50:1238-1244.

14. Chamczynski P, Sacchi N. Single-step method of RNA isolation by acid guanidinium thiocyanate-phenol-chloroform extraction. Anal Biochem 1987;162:156-159.

15. Hall TA. BioEdit: a user-friendly biological sequence alignment editor and analysis program for Windows 95/98/NT. Nucl Acids Symp Ser 1999;41:95-98.

16. 01 September. 2011 MOE, version 2011.10; Chemical Computing Group, Inc. Accessed. Available: www.chemcomp.com/.

17. Laskowski RA, MacArthur MW, Moss DS, Thornton JM. PROCHECK: a program to check the stereochemical quality of protein structures. J Appl Crystallogr 1993;26:283–291.

18. DeLano WL. The PyMOL Molecular Graphics System. DeLano Scientific, San Carlos, CA, USA. 2002 http://www.pymol.org/.

19. Foloppe N, MacKerell Jr AD. All-atom empirical force field for nucleic acids: 1) Parameter optimization based on small molecule and condensed phase macromolecular target data. J Comput Chem 2000;21:86–104.

20. Thomsen R, Christensen MH. MolDock: A new technique for high-accuracy molecular docking. J Med Chem 2006;49:3315-3321.

21. Bond SD, Leimkuhler BJ, Laird BB. The Nose-Poincare method for constant temperature molecular dynamics. J Comp Phys 1999;151:114–134.

22. Cygler M, Schrag JD, Sussman JL, Harel M, Silman I, Gentry MK, Doctor BP. Relationship between sequence conservation and three-dimensional structure in a large family of esterases, lipases and related proteins. Protein Sci 1993;2:366–382.

23. Lockridge O, Adkins S, La Du BN. Location of disulfide bonds within the sequence of human serum cholinesterase. J Biol Chem 1987;262:12945–12952.

24. Kroetz DL, McBride OW, Gonzalez FJ. Glycosylation-dependent activity of Baculovirus-expressed human liver carboxylesterases: cDNA cloning and characterization of two highly similar enzyme forms. Biochemistry 1993;32:11606–11617.

25. Ollis DL, Cheah E, Cygler M, Dijkstra B, Frolow F, Franken SM, Harel M, Remington SJ, Silman I, Schrag J, Sussman JL, Verschueren KHG, Goldman A. The α/β hydrolase fold. Protein Eng 1992;5:197-221.

26. Ben Ali Y, Chahinian H, Petry S, Müller G, Carrière F, Verger R, Abousalham A. Might the kinetic behavior of hormone-sensitive lipase reflect the absence of the lid domain? Biochemistry 2004;43:9298–9306.

27. Yu XW, Tan NJ, Xiao R, Xu Y. Engineering a Disulfide Bond in the Lid Hinge Region of *Rhizopus chinensis* Lipase: Increased Thermostability and Altered Acyl Chain Length Specificity. PLoS ONE 2012;7:e46388.

28. Gatti-Lafranconi P, Natalello A, Rehm S, Doglia SM, Pleiss J, Lotti M. Evolution of stability in a cold-active enzyme elicits specificity relaxation and highlights substrate-related effects on temperature adaptation. J Mol Biol 2010;395:155-166.

29. Brzezinski MR, Abraham TL, Stone CL, Dean RA, Bosron WF. Purification and characterization of a human liver cocaine carboxylesterase that catalyzes the production of benzoylecgonine and the formation of cocaethylene from alcohol and cocaine. Biochem Pharmacol 1994;48:1747-1755.

30. Wang Y, Wei DQ, Wang JF. Molecular Dynamics Studies on T1 Lipase: Insight into a Double-Flap Mechanism. J Chem Inf Model (2010);50:875–878.

31. Cherukuvada SL, Seshasayee ASN, Raghunathan K, Anishetty S, Pennathur G. Evidence of a double-lid movement in *Pseudomonas aeruginosa* lipase: Insights from Molecular Dynamics Simulations. PLoS Comput Biol 2005;1:182–189.

32. Ramakrishnan SK, Krishna V, Kumar KS, Lakshmi BS, Anishetty S, Gautam P. Molecular dynamics simulation of lipases. Int J Integr Biol 2008;2:204–213.

33. Barbe S, Lafaquière V, Guieysse D, Monsan P, Remaud-Siméon M, André I. Insights into lid movements of *Burkholderia cepacia* lipase inferred from molecular dynamics simulations. Proteins 2009;77:509-523.

34. Trodler P, Schmid RD, Pleiss J. Modeling of solvent-dependent conformational transitions in *Burkholderia cepacia* lipase. BMC Struct Biol 2009;9:38-51.

35. Bordes F, Barbe S, Escalier P, Mourey L, André I, Marty A, Tranier S. Exploring the conformational states and rearrangements of *Yarrowia lipolytica* Lipase. Biophys J 2010;99: 2225–2234.

36. Rehm S, Trodler P, Pleiss J. Solvent-induced lid opening in lipases: A molecular dynamics study. Protein Sci 2010;19:2122–2130.

37. Du K, Liu Z, Cui W, Zhou L, Liu Y, Du G, Chen J, Zhou Z. pH-dependent activation of *Streptomyces hygroscopicus* transglutaminase mediated by intein. Appl Environ Microbiol 2014;80:723–729.

38. Verger R. "Interfacial activation" of lipases: facts and artifacts. Trends biotech 1997;15:32-38.

Figure captions

Figure 1. : Nucleotide sequence of the part of the cuCES gene encoding the mature carboxylesterase and the deduced amino acid sequence.

Figure 2. : Alignment of the amino acid sequences of the mature forms of cuCES (this work) and hCES1 [10]. Numbers refer to the amino acid located at the end of each line. Boxes in dark grey indicate positions at which the amino acids are identical in the two carboxylesterases. Boxes in light grey indicate the location of similar residues of the two protein sequences. The closed arrows indicate the Ser, Glu and His which form the catalytic triad. The position of the conserved Cys residues is underlined. (S----S) represents disulfide bridges for human CES1. The additional disulfide bridge of cuCES is shown in red. The dashes represent gaps introduced during the alignment process. Asterisks indicate charge clamp residues. Potential N-glycosylation sites (NAT) and oxyanion hole residues are in blue and yellow, respectively. Homology alignment was performed using the software BioEdit version 7.2.5 [15].

Figure 3. (a) Cartoon representation of the model structure of the chicken uropygial carboxylesterase (cuCES). Secondary structure element labels are indicated and colored by secondary structure succession. The cysteine residues and disulfide bridges are shown as ball and sticks and are indicated. **(b)** and **(c)** Cartoon representation of the first (helix α1) and the second (helix α9) lids of the cuCES. The catalytic residues (Ser202, Glu337 and His452) are shown as sticks. This figure was generated using the PYMOL program [18].

Figure 4. Molecular dynamics simulations and global fluctuations (RMSF) of cuCES during 900 ps of simulation at 310 K and 330 K, respectively.

Figure 5. Model structure of the catalytic pocket of cuCES in complex with a substrate analogue. The substrate analogue (TC_4 analogue) and the catalytic residues (Ser202 and His452) are represented by ball and sticks and indicated. Amino acids interacting with the substrate analogue are represented by sticks and indicated. This figure was generated using the MOE program [16].

Figure 1.

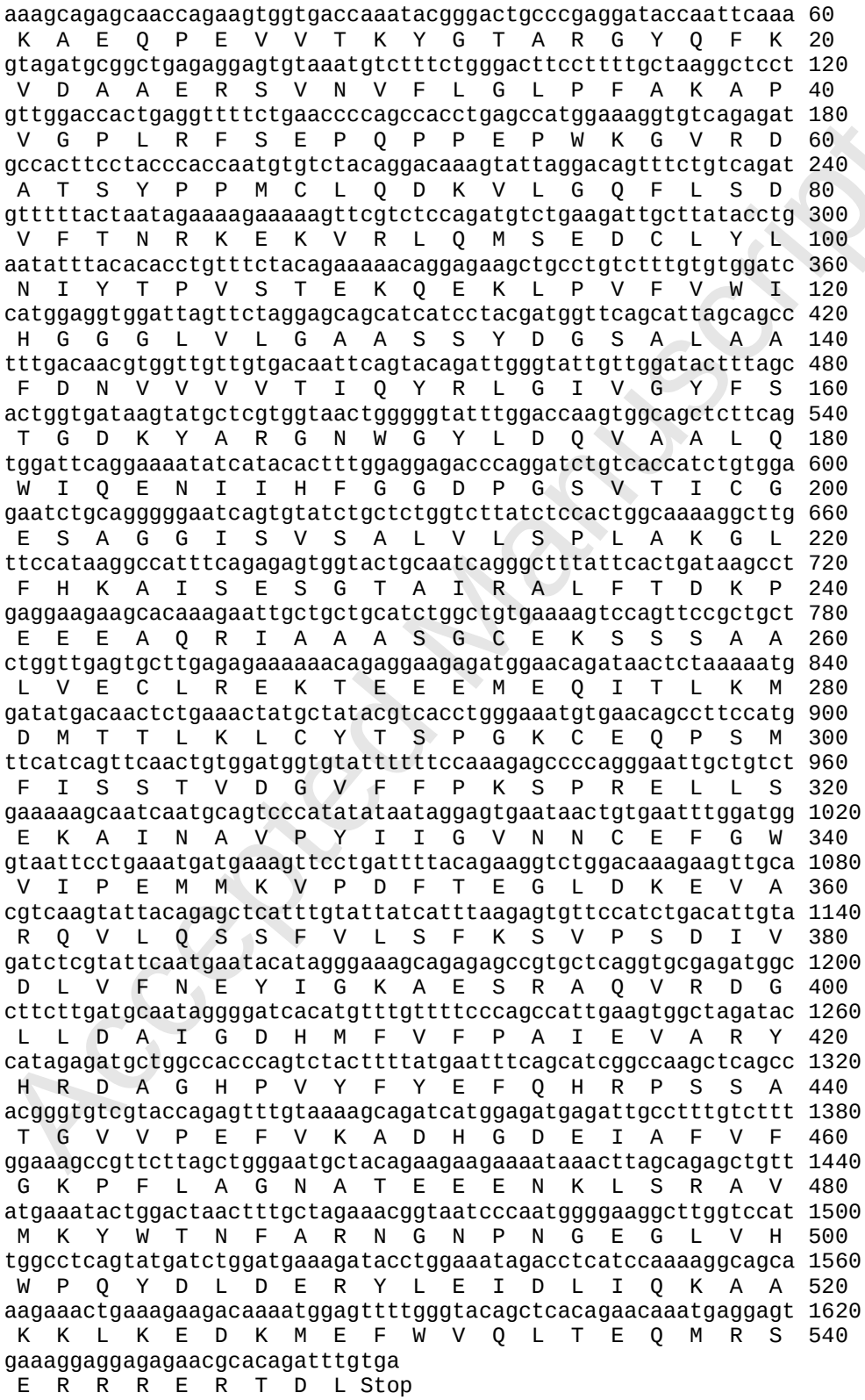

Figure 2.

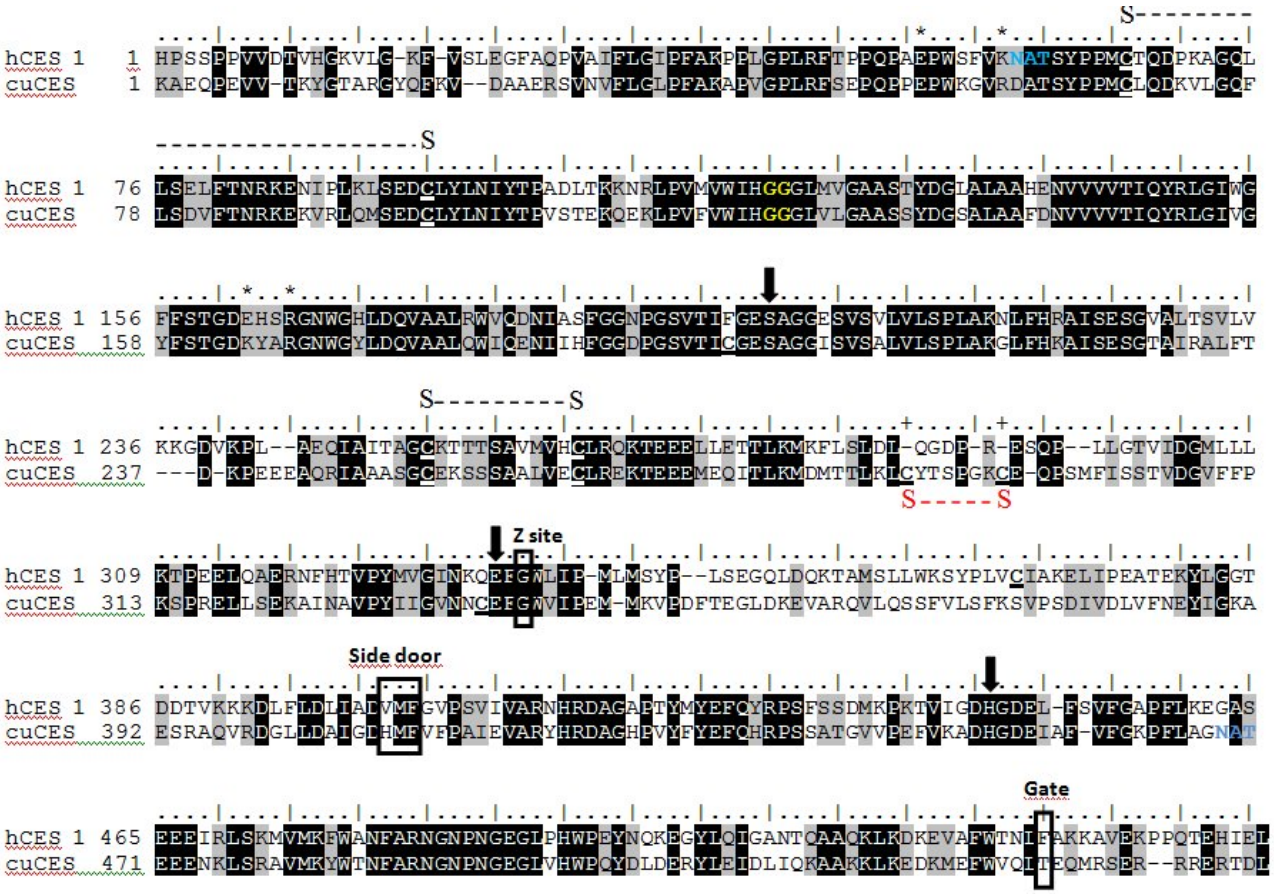

Figure 3.

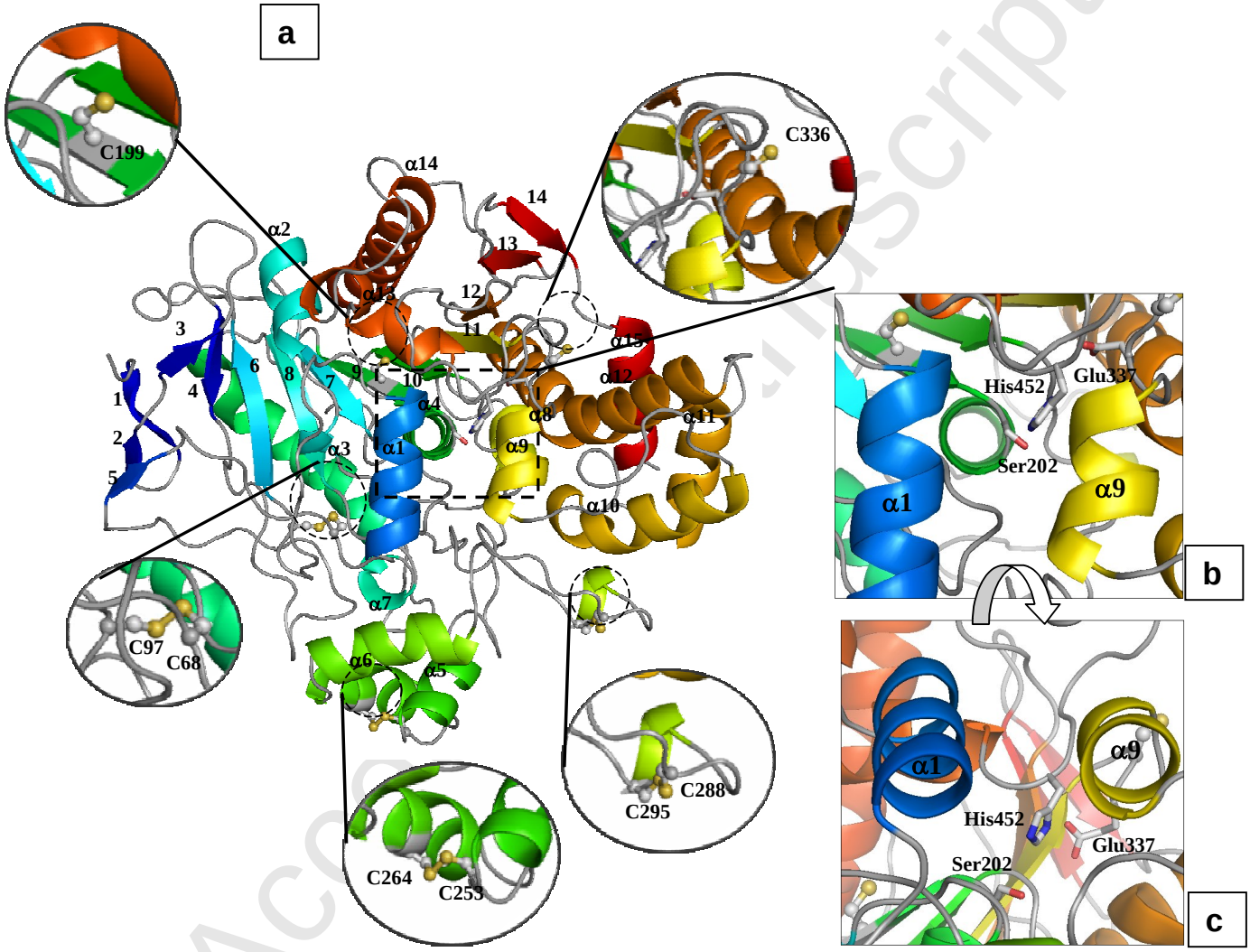

Figure 4.

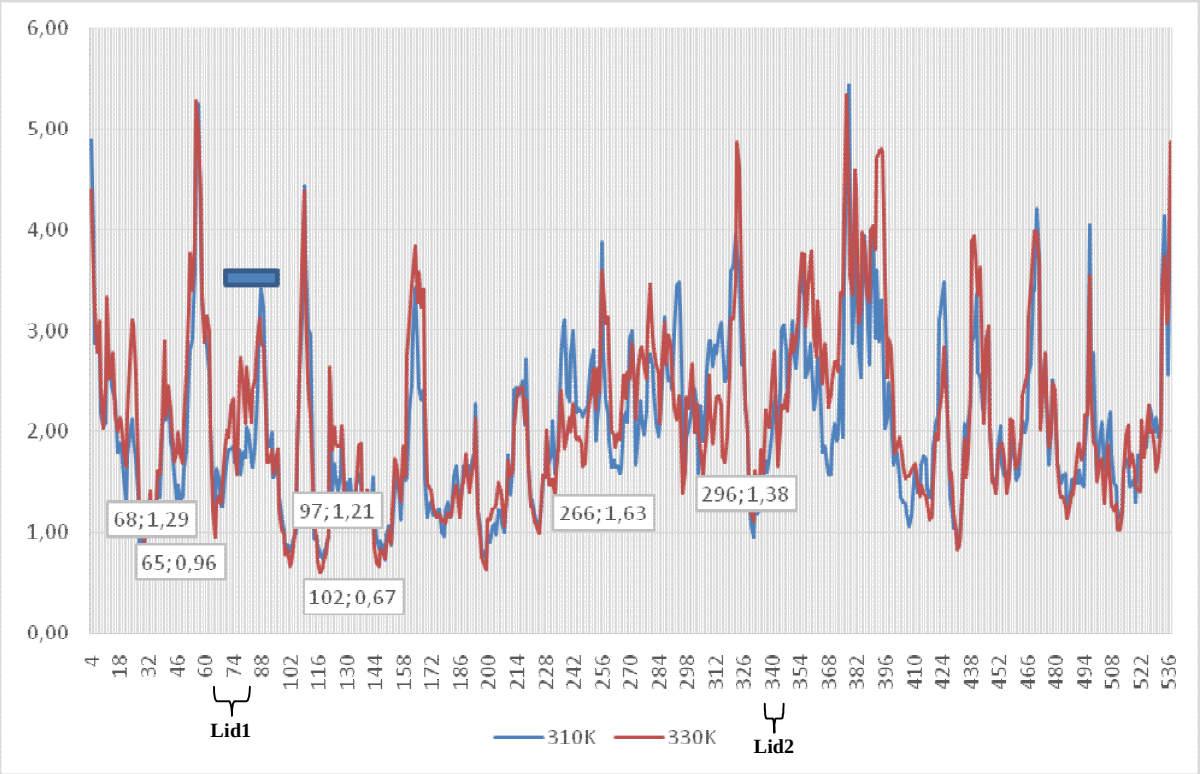

Figure 5.